

Carbon dots serve as an effective probe for the quantitative determination and for intracellular imaging of mercury(II)

Fanyong Yan¹ · Depeng Kong¹ · Yunmei Luo² · Qianghua Ye¹ · Juanjuan He¹ · Xingfei Guo¹ · Li Chen¹

Received: 20 November 2015 / Accepted: 8 February 2016 / Published online: 29 February 2016
© Springer-Verlag Wien 2016

Abstract We describe a new method for synthesis of water-soluble photoluminescent carbon dots (CDs) by one-pot hydrothermal treatment of adipic acid and triammonium citrate. The CDs have excitation/emission maxima of 340/440 nm, a quantum yield of 0.13, and are shown to be a viable fluorescent probe for the determination of Hg(II). It shows a linear relationship in the 4 to 18 μM mercury ion concentration range. The detection limit is as low as 2.47 μM . The CDs were applied to intracellular sensing and imaging of Hg(II) where they showed low toxicity.

Keywords Quenching · Quantum yield · FTIR · X-ray photoelectron spectroscopy · Transmission electron microscopy

Introduction

Mercury ion (Hg(II)) is one of the most toxic heavy metal ions and dangerous pollutants [1–3]. Even in low concentration, it is harmful to the environment and human health. Therefore, it is significant to develop effective analytical methods for sensitive and selective detection of Hg(II). Current Hg(II) detection methods comprise atomic absorption/emission spectroscopy, atomic fluorescence spectrometry, inductively coupled plasma mass spectrometry and polarography [4–6]. Optical probes are valuable because of their high sensitivity and fast analysis. So far, many optical probes have been developed for Hg(II) detection. These include organic molecules, metal nanoclusters, semiconductor quantum dots (QDs) and so on [7–9]. However, the above methods usually suffer from complicated synthesis routes or the use of toxic and expensive reagents. Thus, it is highly desired to develop simple, economical and green strategy to synthesize optical probes.

Carbon nanomaterials have attracted much attention due to their unique properties and potential applications [10]. Compared with conventional organic dyes and semiconductor QDs, fluorescent carbon dots (CDs) are superior because CDs exhibit merits in terms of chemical inertness, lack of blinking, low toxicity and good biocompatibility [11]. CDs can be synthesized without the requirement of complicated preparing steps and passivating agents. Ahmed et al. synthesized hydroxy capped CDs through thermal carbonization method [12]. The fluorescence of the CDs can be significantly quenched by 4-nitrophenol via an energy transfer process. Bhaissare et al. prepared a jelly-like form of CDs by microwave-assisted heating synthesis [13]. The CDs were applied to image HeLa cell lines via the blue fluorescence of the dots. Yang et al. produced CDs through reflux of glucose

Electronic supplementary material The online version of this article (doi:10.1007/s00604-016-1788-5) contains supplementary material, which is available to authorized users.

✉ Fanyong Yan
yfany@163.com

✉ Li Chen
Chenlis@tjpu.edu.cn

¹ State Key Laboratory of Separation Membranes and Membrane Processes, Key Lab of Fiber Modification & Functional Fiber of Tianjin, Tianjin Polytechnic University, Tianjin 300387, People's Republic of China

² Department of pharmacology/Key Laboratory for Basic Pharmacology of Ministry of Education, Zunyi Medical College, Zunyi, Guizhou 563000, People's Republic of China

for the determination of Zn(II) [14]. The CDs were used to establish a fluorescence resonance energy transfer system. This method was also applied to image the distribution of Zn(II) ions in HeLa cells.

A number of significant breakthrough applications of CDs, such as bioimaging, probes, medical diagnosis and photocatalysis have been described [15–18]. The development of cell imaging techniques has drawn much attention [19]. CDs, with sensing capability, are fairly well biocompatible and cell permeable. Thus, CDs can be used as effective fluorescent probes for detecting and intracellular imaging ions. The fluorescent CDs were synthesized by one-pot hydrothermal treatment of adipic acid and triammonium citrate. We investigated the efficient and effective quenching of fluorescence in CDs by heavy metal ions. The CDs can be quenched by Hg(II) at low concentrations. On this basis, the fluorescent probe can be used for the detection of trace Hg(II) in aqueous media. In addition, the CDs were applied to imaging of Hg(II) in living cells and gave satisfying resolution.

Experimental

Chemicals and apparatus

Adipic acid (<http://tjbodi.qianyan.biz/>), triammonium citrate, toluene and ethanol were purchased from local companies (<http://www.tjxhsj.cn/>). Quinine sulfate (99 %) was supplied by Aladdin. Dimethyl sulfoxide (DMSO), fetal bovine serum (FBS), trypsin and 3-(4,5-dimethylthiazol-2-yl)-2,5-diphenyltetrazolium bromide (MTT) were purchased from Solarbio (<http://www.solarbio.net.cn/>). All the other chemicals were analytical grade and used as received. The solutions of metal ions were prepared from NaNO₃, KNO₃, Ba(NO₃)₂, Ce(NO₃)₃, Mn(NO₃)₂, Fe(NO₃)₃, Co(NO₃)₂, Ni(NO₃)₂, PdCl₂, CuCl₂, AgNO₃, Zn(NO₃)₂, Cd(NO₃)₂, Hg(NO₃)₂, Al(NO₃)₃ and Pb(NO₃)₂. The deionized water obtained from a Millipore NanoPure purification system.

Fourier transform infrared (FTIR) spectra were recorded on a TENSOR37 Fourier-transform infrared spectrometer. X-ray photoelectron spectroscopy (XPS) was performed on an X-ray photoelectron spectroscope (EDAX, Genesis 60S). Transmission electron microscopy (TEM) measurements were performed on a Hitachi H-7650 electronic microscope. UV–vis absorption spectra of the samples were recorded on a Purkinje General TU-1901 UV–vis spectrophotometer. Fluorescence emission spectroscopy was carried out on an F-380 fluorescence spectrophotometer. A PHS-3 W pH meter was utilized to measure the pH values of aqueous solutions. The fluorescence imaging was observed under an

Olympus IX71 inverted fluorescence microscope with a 20× objective lens.

Synthesis of CDs

Adipic acid (0.58 g) and triammonium citrate (2.92 g) were dissolved in deionized water (10 mL). Then the solution was transferred to a poly (tetrafluoroethylene) autoclave (15 mL) and heated at 200 °C for 5 h. Then we got transparent brown solution after the reactors cooled down to room temperature. Then, we added sodium hydroxide into the above solution to adjust the pH to 14. The solid was obtained by rotary evaporation and then redissolved in ethanol. The insoluble precipitate in the solution was removed by centrifugation and the supernatant liquid was then used. Then, the solution was further purified through loading into dialysis bags (Mw=3000) for dialysis against distilled water for 4 days. Eventually, pure CDs were obtained by rotary evaporation.

Detection of Hg(II)

For the typical assay, CDs were dispersed in double distilled water to get 2.5 mg mL⁻¹ aqueous solution. Standard aqueous solutions of NaNO₃, KNO₃, Ba(NO₃)₂, Ce(NO₃)₃, Mn(NO₃)₂, Fe(NO₃)₃, Co(NO₃)₂, Ni(NO₃)₂, PdCl₂, CuCl₂, AgNO₃, Zn(NO₃)₂, Cd(NO₃)₂, Hg(NO₃)₂, Al(NO₃)₃ and Pb(NO₃)₂ were prepared in water with concentration of 2 mM. In a typical detection experiment, 0.1 mL CD solution was added into a certain amount of metal ions solution to form a 10 mL clear solution with water. All samples were prepared at room temperature. After mixing evenly, fluorescence measurements were carried out with excitation and emission slit width of 5 and 10 nm and excitation wavelength of 360 nm.

Experimental details for cell imaging experiments

HUVEC cells were cultured in medium supplemented with 10 % fetal bovine serum (FBS, Invitrogen) at 37 °C under an atmosphere containing 5 % CO₂. For imaging, HUVEC cells were seeded on a coverslip in 6-well plate 12 h before use. The culture medium was replaced by 2.5 mL fresh medium containing 10 µg mL⁻¹ CDs and the cells were incubated for another 24 h. After being washed with fresh phosphate buffer (pH=7.0) three times, the cells were imaged on the inverted fluorescence microscope. For intracellular sensing and imaging of Hg(II), the culture medium was replaced by 2.5 mL fresh medium containing 10 µg mL⁻¹ CDs. Then the cells were firstly incubated for 24 h and secondly incubated with 20 µM Hg(II) for another 0.5 h at 37 °C. The cells were imaged again after washing the culture medium three times with phosphate buffer.

Results and discussion

Choice of materials

In the reported methods, the oxidation of gas soot, carbon soot or activated carbon requires the presence of strong acids, which are undesirable and hazardous [20–23]. In addition, carbonization of glucose, citric acid, ascorbic acid, etc. to synthesize fluorescent CDs needs multi-step operations and strong acids. They often need post-treatments with surface passivated agents to improve the water solubility and luminescence properties. Much effort has been made to obtain self-passivated carbon dots through high temperature or microwave-assisted hydrothermal treatment [24–26]. It is still

highly desired to explore carbon source for simple, economical and green synthesis of CDs. Adipic acid is the most useful fatty binary acid, which can take part in the reaction of salt-forming, esterification, acylation and polycondensation with diamines. Triammonium citrate contains both carbon and nitrogen. CDs were prepared by hydrothermal method using adipic acid as the carbon source and triammonium citrate as the surface passivation agent.

In order to get high-quality CDs, the synthesis conditions, such as different ratios of adipic acid and triammonium citrate, reaction temperature and time, were optimized (Tables S1, Table S2). The QY increases with the hydrothermal reaction temperature and time and reaches a stable value when the temperature was beyond 200 °C. CDs with the highest QY

Fig. 1 TEM image and HRTEM image (inset) of CDs (a). FTIR spectrum of CDs (b). XPS survey scan of CDs (c). The enlarged regions for C1s, N1s, O1s of CDs (d, e, f)

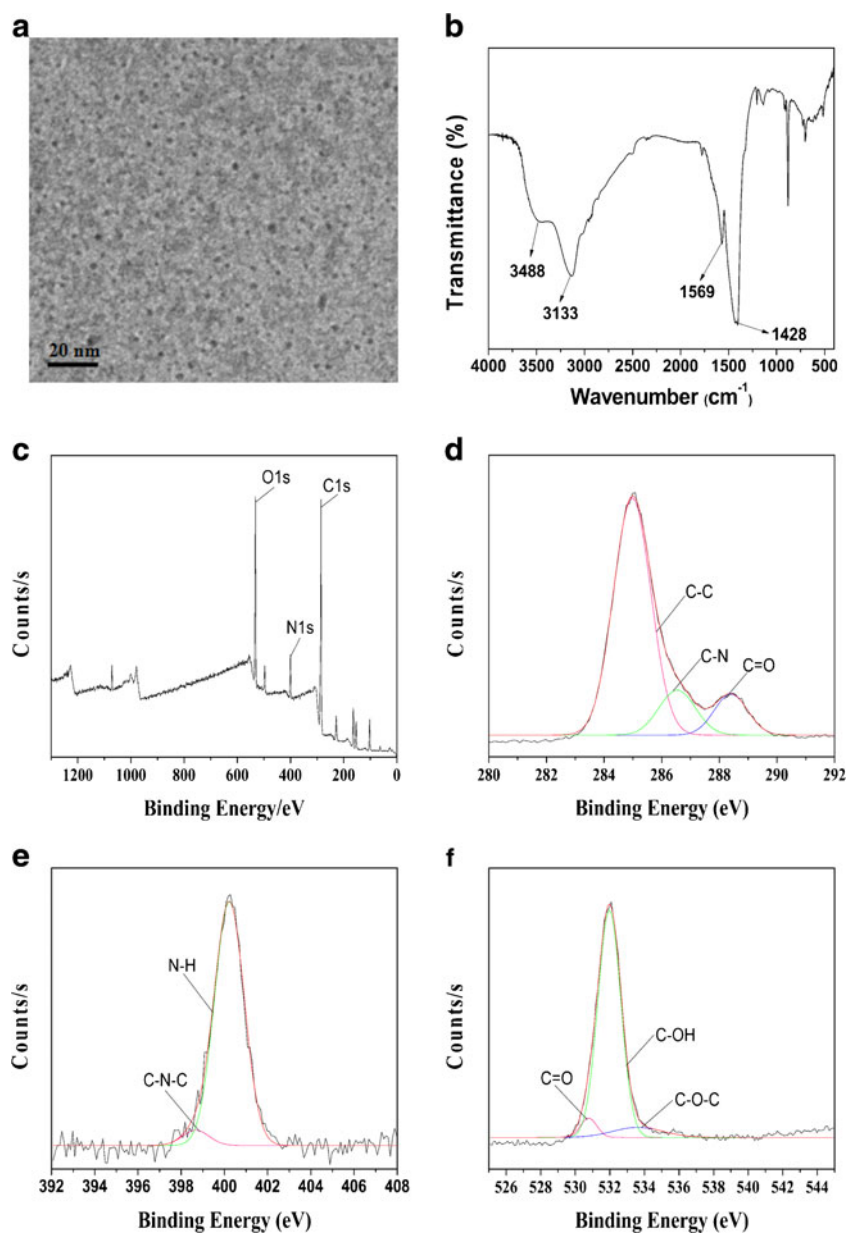
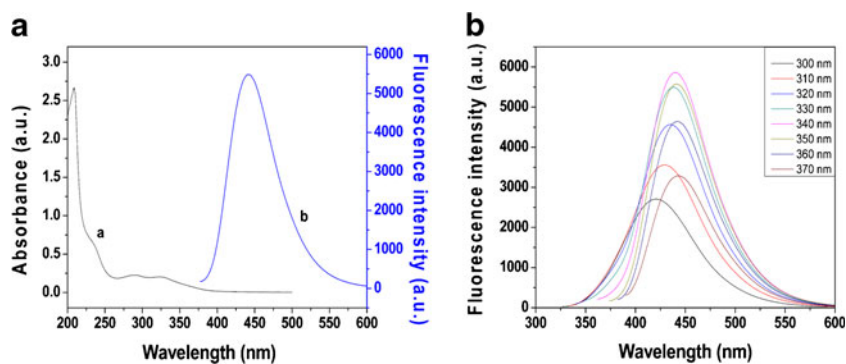


Fig. 2 Absorption and fluorescence emission spectra of CDs (a). Fluorescence spectra (exCitation wavelength from 300 to 370 nm in 10 nm increments) of CDs (b)



can be obtained from hydrothermal reaction of adipic acid (0.58 g) and triammonium citrate (2.92 g) at 200 °C for 5 h. The CDs have lower QY with lower reaction temperature and time. Besides, non-fluorescent carbon nanoparticles were obtained with even higher reaction temperature or more time.

Characterization of CDs

TEM was applied to investigate the morphologies of the prepared CDs. Figure 1a shows that CDs are monodisperse with near spherical morphologies. Based on the statistical analysis of particles, the average size is about 3.9 ± 0.5 nm. The size distribution of CDs was calculated by measuring approximately 150 particles from TEM image of CDs (Fig. S1). The high-resolution TEM (HRTEM) picture in Fig. 1a reveals that the CDs have a lattice spacing of approximately 0.32 nm, which is consistent with the (002) planes of graphitic carbon [27]. FTIR was used to further study the surface functional groups of CDs (Fig. 1b). The peaks at 3488 cm^{-1} and 3133 cm^{-1} come from the stretching vibrations of O-H and N-H. It reveals a large quantity of hydroxy and amino groups on the surface of CDs. These results demonstrate the water-solubility of CDs. Furthermore, the other two peaks around 1569 cm^{-1} and 1428 cm^{-1} are originated from C=O and C-N, respectively. Then we performed XPS to analyze the composition and surface elements of CDs (Fig. 1c). The XPS survey

spectrum of the CDs shows three main peaks at 285, 400 and 532 eV, which are ascribed to C1s, N1s and O1s, respectively. The high resolution C1s reveals three peaks center at 285, 286, 288 eV, attributing to the binding energy of C–C, C–N and C=O (Fig. 1d). This indicates the existence of carbon atoms connecting to N and O heteroatoms. The N1s spectrum shows two peaks around 400 eV, which are assigned to the C–N–C and N–H bands, respectively (Fig. 1e). The spectrum of O1s is split into three peaks coming from the binding energy of C=O, C–OH and C–O–C (Fig. 1f) [28, 29]. These results are consistent with the above FTIR spectra conclusions.

The optical properties of CDs were studied through UV–Vis absorption and fluorescence spectroscopy (Fig. 2). As shown in Fig. 2a, CDs showed strong absorbance in the deep UV (210 nm), which was ascribed to the π – π^* transition of aromatic sp^2 domains [30]. The other peak centered at 330 nm indicated the n – π^* transition of C=O [31]. Figure 2b reveals the fluorescence emission spectra of CDs. We used 300 to 370 nm excitation wavelengths ranging by 10 nm increment. The fluorescence intensity increases initially till 340 nm and then decreases gradually by changing the excitation wavelength from lower to higher. We performed all the experiments at 340 nm excitation wavelength. Moreover, the fluorescence quantum yield was about 13.33 %, using quinine sulfate (54 % in $0.1 \text{ mol L}^{-1} \text{ H}_2\text{SO}_4$, $\lambda_{\text{ex}} = 371 \text{ nm}$) as a reference material (see the detail in Supporting information).

Fig. 3 Effect of metal ions on the fluorescence intensity of CDs (a). Fluorescence emission spectra of CDs in the absence and presence of ($12 \mu\text{M}$) Hg(II) (b)

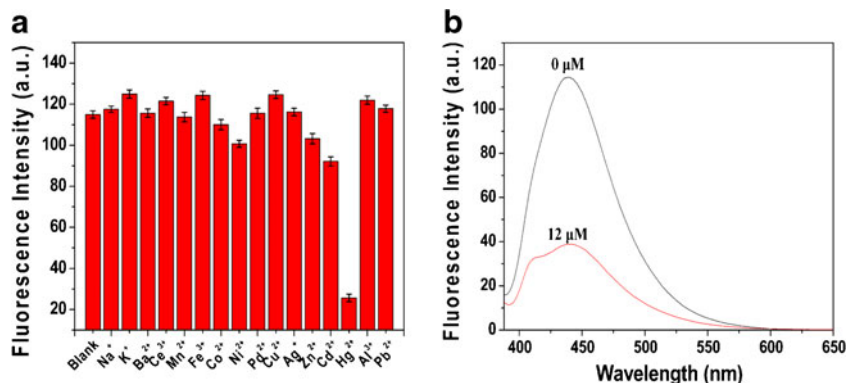


Table 1 Comparison of different carbon dots for Hg(II) detection

Carbon dots	Materials	Quantum yield (%)	Quenching ratio (%)	Ref.
1	Flour	5.4	27 (40 μM)	[7]
2	Formamide	29	50 (9 μM)	[8]
3	Citric acid and 1,2-ethylenediamine	43.8	40 (20 μM)	[9]
4	Adipic acid and triammonium citrate	13.3	70 (12 μM)	This work

Feasibility of CDs in the detection of Hg(II)

The fluorescence intensity changes of CDs were performed in the presence of most common metal ions under the same condition. As shown in Fig. 3a, a much lower fluorescence was found in the presence of Hg(II). In contrast, no obvious decrease was discovered by adding the other metal ions into the CD solution. It can be obviously seen that CDs exhibit a strong fluorescence peak around 440 nm in the absence of Hg(II). While after the addition of 12 μM Hg(II), nearly 70 % of the fluorescent intensity is quenched (Fig. 3b). Table 1 compares the performances of different kinds of CDs for Hg(II) detection. This result indicates that our fluorescent probe provides an efficient method for detecting Hg(II).

Quenching mechanism and quantitative analysis of Hg(II)

As mentioned above, the CDs were capped with amino groups and carboxy groups. Initially, the free CDs showed strong fluorescence in aqueous solution. However, the fluorescence of CDs was quenched obviously in the presence of Hg(II) (Fig. 4). It is speculated that the fluorescence emission of CDs comes from the radiative recombination of excitons, which is similar to QDs. The outstanding specificity is

attributed to the stronger affinity between Hg(II) and carboxy groups of CDs. Then it facilitates the non-radiative electron/hole recombination annihilation via effective electron transfer process and quenches the fluorescence of CDs [32, 33].

To further study the interaction between Hg(II) and CDs, the fluorescence sensing behavior of CDs for Hg(II) was explored. Under the same conditions, different concentrations of Hg(II) were added into the CD solution. The fluorescent intensity of CDs at 438 nm gradually decreased by increasing the Hg(II) concentration. From the corresponding linear plot (Fig. 5a), it can be concluded that the linear range is from 4 to 18 μM . The calibration curve can be expressed as $F_0/F-1=0.2537+0.2537c$ with correlation coefficient of 0.9965. F_0 and F are the fluorescent intensities of CDs in the absence and presence of Hg(II). The detection limit was calculated to be 2.47 μM based on $3\sigma/s$ (σ is the standard deviation of eight blank measurements, s is the slope of the calibration curve). Potential interferences from other metal cations were investigated to study the special recognition of Hg(II) by CDs. The fluorescent intensity changes of CDs in the presence of 20 μM of Hg(II) occurred with other common metal ions under the same concentration. Figure 5b shows that the fluorescence changes of CDs towards Hg(II) in the presence of other competitive metal ions are negligible. A performance comparison of the methods for the analysis of Hg(II) from this work with

Fig. 4 Schematic illustration for the synthesis of CDs and their applications in the determination and intracellular imaging Hg(II)

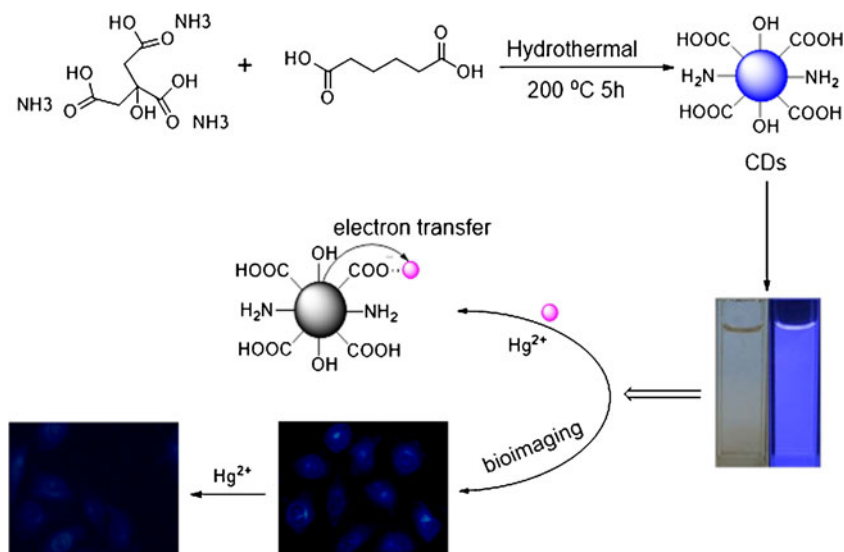
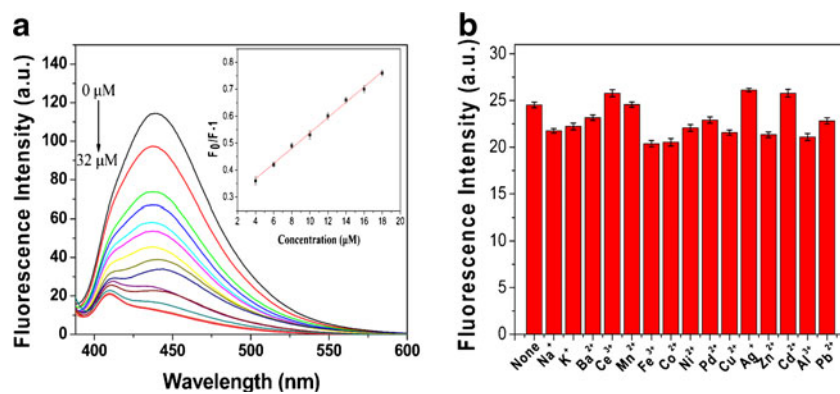


Fig. 5 Fluorescence emission spectra of CDs in the presence of different concentrations of Hg(II) (from 0 to 32 μM), inset shows the dependence of $F_0/F-1$ on the concentrations of Hg(II) (a). Fluorescence response of CDs in the presence of 20 μM of Hg(II) with the addition of different metal ions under the same concentration (b)



that from some other studies was studied (Table 2). It reveals that this method has high sensitivity, good linear response range and comparable detection limit to that found in other studies. These results suggest that the prepared CDs can be developed as an effective fluorescent probe for Hg(II) sensing.

Applications

For cells and living organisms, UV excitable probes may show some limitations due to the scattering of excitation and emission light and auto-fluorescence [38]. Actually, the fluorescent CDs may cause some back ground luminescence by biomatter when excited by UV light. But the CDs possess excellent optical properties in the field of broad excitation spectra and tunable emission wavelength which can be superiorly used in biological system. The feasibility of CDs as bioimaging agents in bean sprouts was investigated to evaluate their cytotoxicity. The beans grown in 1 mg mL⁻¹ CD solution are similar to the bean sprouts grown in water. Under UV light, sprouts exhibited strong blue luminescence, indicating that the CDs permeate into the cells and do not adversely affect plant growth (Fig. S2). To further study the cytotoxicity of CDs, a MTT assay on HUVEC cells with CD concentrations from 0 to 200 $\mu\text{g mL}^{-1}$ was explored. Figure S3 shows the cytotoxicity data of CDs with different concentrations. According to the assay, CDs did not obviously reduce cell viability. Based on the viability data from MTT assay, it can be seen that CDs present low toxicity.

Table 2 Figures of merit of recently reported methods for determination of Hg(II)

Methods	Linear range (μM)	Detection limit (μM)	Ref.
TFIC MNPs	4–16	5.04	[34]
L-Cys-GNPs	100–2000	100	[35]
AuNC–CdTe QD	131–710	9	[36]
CDs	0–3000	4.2	[37]
CDs	4–18	2.47	This work

Then the response of the probe to Hg(II) in the cultured cells was explored to investigate the application of this probe for Hg(II) detection in biological system. Figure 6b displays photographs of the HUVEC cells captured by a laser scanning confocal microscope. The transfected HUVEC cells became quite bright blue owing to the strong fluorescence from CDs. It indicates that a large amount of CDs have been internalized into the cells. In addition, the bright-field image of the HUVEC cells incubated with CDs/Hg(II) clearly reveals the normal morphology of the cells. It verifies that CDs/Hg(II) are biocompatible and possess minimum toxicity to the cells (Fig. 6c). The cells incubated with CDs/Hg(II) display weaker emission than the CDs, probably because Hg(II) ions quench the fluorescence of CDs. As such, CDs can be used as an effective fluorescent probe for monitoring Hg(II) in bio-system.

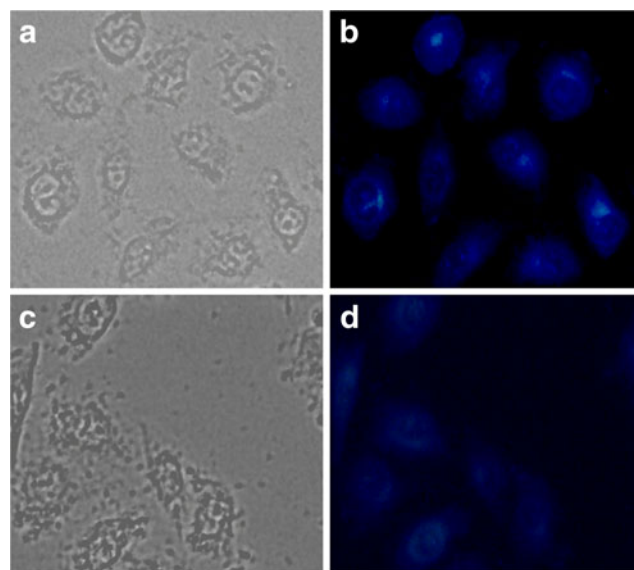


Fig. 6 Bright-field transmission image (a) and fluorescence image (b) of HUVEC cells incubated with CDs for 24 h at 37 °C. Bright-field transmission image (c) and fluorescence image (d) of HUVEC cells incubated with CDs for 24 h and then incubated with Hg(II) for about 0.5 h at 37 °C. Scale bar: 20 μm

Conclusions

CDs with high remarkable fluorescence properties were synthesized and found to be “turn-off” fluorescence probe for Hg(II) detection. Because of the strong affinity between Hg(II) and carboxy groups of CDs, the fluorescence was quenched through effective electron transfer process. Although the probe may cause strong back ground luminescence by any biomatter when excited at 360 nm, the CDs with broad excitation spectra and tunable emission wavelength can also be applied to intracellular sensing and imaging of Hg(II). Therefore, it offers opportunities that range from experimental research to practical applications. It also provides a promising tool in fluorescent bioimaging and biosensing.

Acknowledgments The work described in this manuscript was supported by the National Natural Science Foundation of China (Nos. 21174103, 21374078, 51308390) and Tianjin Research Program of Application Foundation and Advanced Technology (No. 15JCYBJC18100).

Compliance with ethical standards The author(s) declare that they have no competing interests.

References

1. Yan FY, Zou Y, Wang M, Mu XL, Yang N, Chen L (2014) Highly photoluminescent carbon dots-based fluorescent chemosensors for sensitive and selective detection of mercury ions and application of imaging in living cells. *Sensors Actuators B* 192:488–495
2. Nolan EM, Lippard SJ (2003) A “turn-on” fluorescent sensor for the selective detection of mercuric ion in aqueous media. *J Am Chem Soc* 125:14270–14271
3. Nolan EM, Lippard SJ (2005) MS4, a seminaphthofluorescein-based chemosensor for the ratiometric detection of Hg(II). *J Mater Chem* 15(27):2778–2783
4. Leopold K, Foulkes M, Worsfold P (2010) Methods for the determination and speciation of mercury in natural waters—a review. *Anal Chim Acta* 663:127–138
5. Gong Y, Zhang X, Chen Z, Yuan Y, Jin Z, Mei L, Zhang J, Tan W, Shen G, Yu R (2012) An efficient rhodamine thiospirolactambased fluorescent probe for detection of Hg(II) in aqueous samples. *Analyst* 137(4):932–938
6. Lin Y, Tseng WL (2010) Ultrasensitive sensing of Hg(II) and CH_3Hg^+ based on the fluorescence quenching of lysozyme type VI-stabilized gold nanoclusters. *Anal Chem* 82(22):9194–9200
7. Qin XY, Lu WB, Asiri AM, Al-Youbi AO, Sun XP (2013) Microwave-assisted rapid green synthesis of photoluminescent carbon nanodots from flour and their applications for sensitive and selective detection of mercury(II) ions. *Sensors Actuators B* 184: 156–162
8. Barman S, Sadhukhan M (2012) Facile bulk production of highly blue fluorescent graphitic carbon nitride quantum dots and their application as highly selective and sensitive sensors for the detection of mercuric and iodide ions in aqueous media. *J Mater Chem* 22(41):21832–21837
9. Du FK, Zeng F, Ming YH, Wu SZ (2013) Carbon dots-based fluorescent probes for sensitive and selective detection of iodide. *Microchim Acta* 180(5):453–460
10. Bourlinos A, Trivizas G, Karakassides M, Baikousi M, Kouloumpis A, Goumis D, Bakandritsos A, Hola K, Kozak O, Zboril R, Papagiannouli I, Aloukos P, Couris S (2015) Green and simple route toward boron doped carbon dots with significantly enhanced non-linear optical properties. *Carbon* 83:173–179
11. Baker SN, Baker GA (2010) Luminescent carbon nanodots: emergent nanolights. *Angew Chem Int Ed* 49(38):6726–6744
12. Ahmed G, Laiño R, Calzón G, García M (2015) Highly fluorescent carbon dots as nanoprobes for sensitive and selective determination of 4-nitrophenol in surface waters. *Microchim Acta* 182(1):51–59
13. Bhaiare ML, Talib A, Khan MS, Pandey S, Wu HF (2015) Synthesis of fluorescent carbon dots via microwave carbonization of citric acid in presence of tetraoctylammonium ion, and their application to cellular bioimaging. *Microchim Acta* 182(13): 2173–2181
14. Yang MM, Kong WQ, Li H, Liu J, Huang H, Liu Y, Kang ZH (2015) Fluorescent carbon dots for sensitive determination and intracellular imaging of zinc(II) ion. *Microchim Acta* 182(15):2443–2450
15. Hou JY, Dong J, Zhu HS, Teng X, Ai SY, Mang ML (2015) A simple and sensitive fluorescent sensor for methyl parathion based on L-tyrosine methyl ester functionalized carbon dots. *Biosens Bioelectron* 68:20–26
16. Zhang PJ, Xue ZJ, Luo D, Yu W, Guo ZH, Wang T (2014) Dual-Peak electrogenerated chemiluminescence of carbon dots for iron ions detection. *Anal Chem* 86(12):5620–5623
17. Zou Y, Yan FY, Zheng TC, Shi DC, Sun FZ, Yang N, Chen L (2015) Highly luminescent organosilane-functionalized carbon dots as a nanosensor for sensitive and selective detection of quercetin in aqueous solution. *Talanta* 135:145–148
18. Yang ST, Cao L, Luo PG, Lu FS, Wang X, Wang HF, Meziari MJ, Liu YF, Qi G, Sun YP (2009) Carbon dots for optical imaging in vivo. *J Am Chem Soc* 131:11308–11309
19. Wolfbeis O (2015) An overview of nanoparticles commonly used in fluorescent bioimaging. *Chem Soc Rev* 44(14):4743–4768
20. Liu HP, Ye T, Mao CD (2007) Fluorescent carbon nanoparticles derived from candle soot. *Angew Chem Int Ed* 46(34):6473–6475
21. Qiao ZA, Wang YF, Gao Y, Li HW, Dai TY, Liu YL, Huo QS (2010) Commercially activated carbon as the source for producing multicolor photoluminescent carbon dots by chemical oxidation. *Chem Commun* 46(46):8812–8814
22. Sun YP, Zhou B, Lin Y, Wang W, Fernando KAS, Pathak P, Meziari MJ, Harruff BA, Wang X, Wang HF, Luo PJG, Yang H, Kose ME, Chen BL, Veca LM, Xie SY (2006) Quantum-sized carbon dots for bright and colorful photoluminescence. *J Am Chem Soc* 128(24):7756–7757
23. Tian L, Ghosh D, Chen W, Pradhan S, Chang XJ, Chen SW (2009) Nanosized carbon particles from natural gas soot. *Chem Mater* 21(13):2803–2809
24. Hsu PC, Chang HT (2012) Synthesis of high-quality carbon nanodots from hydrophilic compounds: role of functional groups. *Chem Commun* 48(33):3984–3986
25. Sahu S, Behera B, Maiti TK, Mohapatra S (2012) Simple one-step synthesis of highly luminescent carbon dots from orange juice: application as excellent bio-imaging agents. *Chem Commun* 48(70):8835–8837
26. Yang ZC, Wang M, Yong AM, Wong SY, Zhang XH, Tan H, Chang AY, Li X, Wang J (2011) Intrinsically fluorescent carbon dots with tunable emission derived from hydrothermal treatment of glucose in the presence of monopotassium phosphate. *Chem Commun* 47(42): 11615–11617
27. Li HT, He XD, Kang ZH, Huang H, Liu Y, Liu JL, Lian SY, Tsang CA, Yang XB, Lee ST (2010) Water-soluble fluorescent carbon quantum dots and photocatalyst design. *Angew Chem Int Ed* 49(26):4430–4434

28. Ahmed MJ, Hossan J (1995) Spectrophotometric determination of aluminium by morin. *Talanta* 42:1135–1142
29. Li YF, Liu Y, Zhou M (2012) Synthesis and properties of a dendritic FRET donor–acceptor system with cationic iridium(III) complex core and carbazolyl periphery. *Dalton Trans* 41(9):2582–2591
30. Ray SC, Saha A, Jana NR, Sarkar R (2009) Fluorescent carbon nanoparticles: synthesis, characterization, and bioimaging application. *J Phys Chem C* 113:18546–18551
31. Hu SL, Niu KY, Sun J, Yang J, Zhao NQ, Du XW (2009) One-step synthesis of fluorescent carbon nanoparticles by laser irradiation. *J Mater Chem* 19(4):484–488
32. Chai F, Wang T, Li L, Liu H, Zhang L, Su Z, Wang C (2010) Fluorescent gold nanoprobe for the sensitive and selective detection of Hg(II). *Nanoscale Res Lett* 5(11):1856–1860
33. Wang H, Wang Y, Jin J, Yang R (2008) Gold nanoparticle-based colorimetric and turn-on fluorescent probe for mercury(II) ions in aqueous solution. *Anal Chem* 80(23):9021–9028
34. Niu LY, Guan YS, Chen YZ, Wu LZ, Tung CH, Yang QZ (2012) BODIPY-based ratiometric fluorescent sensor for highly selective detection of glutathione over cysteine and homocysteine. *J Am Chem Soc* 134:18928–18931
35. Chai F, Wang CG, Wang TT, Ma ZF, Su ZM (2010) L-cysteine functionalized gold nanoparticles for the colorimetric detection of Hg(II) induced by ultraviolet light. *Nanotechnology* 21:025501
36. Paramanik B, Bhattacharyya S, Patra A (2013) Detection of Hg(II) and F⁻ ions by using fluorescence switching of quantum dots in an Au-Cluster–CdTe QD nanocomposite. *Chem Eur J* 19:5980–5987
37. Zhou L, Lin YH, Huang ZZ, Ren JS, Qu XG (2012) Carbon nanodots as fluorescence probes for rapid, sensitive, and label-free detection of Hg(II) and biothiols in complex matrices. 48: 1147–1149
38. Staudinger C, Borisov SM (2015) Long-wavelength analyte-sensitive luminescent probes and optical (bio) sensors. *Methods Appl Fluoresc* 3:042005